Available online at www.sciencedirect.com
SCIENCE DIRECT®
Journal of Sound and Vibration 291 (2006) 1122–1147
JOURNAL OF SOUND AND VIBRATION
www.elsevier.com/locate/jsvi

A unified approach for the free vibration analysis of an elastically supported immersed uniform beam carrying an eccentric tip mass with rotary inertia

Jong-Shyong Wu*, Shou-Hsiung Hsu

Department of Naval Architecture and Marine Engineering, National Cheng-Kung University, Tainan 701, Taiwan, ROC

Received 26 October 2004; received in revised form 20 May 2005; accepted 12 July 2005
Available online 15 September 2005

Abstract

Although an immersed beam with elastic support and fixed support are usually tackled, separately, to simplify the procedures of analysis, a unified approach will be more convenient for the computer programming in the computer method. The purpose of this paper is to use a unified approach to determine the ''exact'' lowest several natural frequencies and the associated mode shapes of the (partially or fully) immersed beam in both the elastic- and fixed-support conditions. Furthermore, by modeling the distributed added mass along the immersed part of the beam with a number of concentrated added masses, a point added mass method (PAM) incorporated with the mode-superposition approach is also presented to determine the ''approximate'' lowest several natural frequencies and the associated mode shapes of the last two types of immersed beam. It is unlike most of the vibrating systems with their boundary conditions independent on the eigenvalues that the boundary conditions of the current immersed beam are frequency dependent due to the existence of frequency-dependent boundary inertial forces and moments. Since the last frequency-dependent boundary conditions significantly affect the orthogonal condition of the mode shapes and so do the applicability of the mode-superposition approach for the vibration analysis, the theory regarding the orthogonal condition for the mode shapes of the current vibrating system will be one of the key points in this paper. The numerical results have been compared with the existing information or the results of finite element method and a good agreement is achieved. Furthermore, to check the last

*Corresponding author. Tel.: +886 6 258 7376; fax: +886 6 280 8458.
E-mail address: jswu@mail.ncku.edu.tw (J.-S. Wu).

0022-460X/$ - see front matter
doi:10.1016/j.jsv.2005.07.032

theoretical results, several model tests are also carried out on the scale models of the fixed and elastically supported towers and reasonable agreement is obtained.

1. Introduction

Since the dynamic characteristics of some structures, such as towers, piles, tall buildings and robot arms, can be predicted with a reasonable accuracy from an elastically (or fixedly) supported beam carrying a tip mass with (or without) rotary inertia, a lot of researchers devoted themselves to the study of problems in this aspect. For the free vibration analysis of "uniform" beam with tip mass, Refs. [1–14] are some of the pertinent literature and for that of "non-uniform" beam with tip mass, Refs. [15–20] are the associated articles. Refs. [21,22] regarding the forced vibration responses of tower due to wave excitation and earthquake may be also the pertinent literature for some researchers. Among the above-mentioned literature, only the most concerned references will be reviewed here. In Ref. [19], Chang and Liu studied the natural frequencies of immersed restrained column by means of the transfer matrix method. Their purpose is to study the influence of the following parameters: taper ratio of the beam, magnitudes of tip mass, eccentricity and rotary inertia, axial load, and the stiffness of elastic-support translational and rotational springs. Although most of the problem concerned has been studied in Ref. [19], the approach used is a conventional "approximate" method. For this reason, Uscilowska and Kolodziej [13] presented an analytical method to determine the "exact" lowest five natural frequencies and mode shapes of the uniform cantilever tower carrying an eccentric tip mass with mass moment of inertia. Recently, in Ref. [14], the same problem as Ref. [13] is studied by Oz. There, the numerical results of the conventional finite element method (FEM) are used to check the analytical (exact) solutions.

In reality, the support condition of an offshore tower is elastic rather than completely fixed. Hence, it will be more reasonable to model the interactions between tower and soil by using a translational (helical) spring and a rotational spring. In other words, the actual support condition for the lower end of an offshore tower will be close to the condition between soft-spring support and fixed support. In such a situation, two types of tower must be considered, one is elastically supported and the other is fixedly supported. The purpose of this paper is to use a unified approach to determine the "exact" lowest several natural frequencies and the associated mode shapes of the last two types of (partially or fully) immersed beam. Furthermore, since determination of the "exact" natural frequencies and mode shapes of an immersed column with intermediate (in-span) lumped masses is usually difficult no matter whether the column is uniform or non-uniform, this paper also presents the point added mass method (PAM) [20] incorporated with the analytical-and-numerical combined method (ANCM) [7] to solve the title problem. It is noted that the PAM and the ANCM are available only if the mode shapes of the vibrating system are orthogonal. One of the main differences between the vibrating system of this paper and those of Refs. [7,20] is that the boundary conditions of the former are frequency dependent and those of the latter have nothing to do with the eigenvalues. For this reason, the orthogonal condition of mode shapes of the current vibrating system is more complicated than those of Refs. [7,20].

Besides, the analytical (exact) method is available only for the immersed column without carrying any intermediate (in-span) realistic lumped masses, but both the PAM and the FEM are available for the immersed column with or without carrying any number of intermediate lumped masses. A good agreement between the results of analytical (exact) method, PAM and FEM confirms the reliability of the presented approaches. For convenience, in this paper, the immersed beam (in contact with water) is also called the "wet" beam, and it is evident that the "dry" beam (without contact with water) is the special case of the "wet" beam.

2. Natural frequencies and mode shapes of an immersed (wet) beam

For the uniform Euler–Bernoulli beam shown in Fig. 1, the equation of motion of the immersed part is given by [13,23]

$$EIy_1''''(x,t) + (\rho + \rho_w)A\ddot{y}_1(x,t) = 0 \quad \text{for } 0 \leqslant x \leqslant L_1, \tag{1}$$

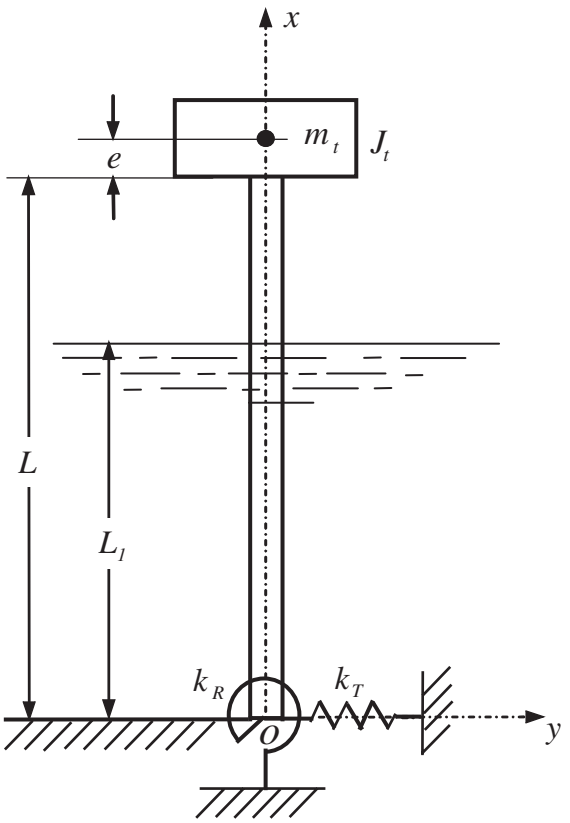

Fig. 1. A partially immersed beam carrying a tip mass m_t with mass moment of inertia J_t and eccentricity e, and supported by a translational spring k_T and a rotational spring k_R.

where E is Young's modulus, A is cross-sectional area, I is moment of inertia of area A, ρ is mass density of beam, ρ_w is mass density of water, x is the axial coordinate with origin at the lower end of the beam, $y_1(x,t)$ is the lateral displacement at x and time t. Besides, in Eq. (1), the primes ($'$) refer to the derivatives with respect to (w.r.t.) coordinate x and the over dots ($\cdot$) refer to those w.r.t. time t.

It is evident that the equation of motion for the emerged part of the beam may be obtained from Eq. (1) by setting $\rho_w = 0$, i.e.,

$$EIy_2''''(x,t) + \rho A\ddot{y}_2(x,t) = 0 \quad \text{for } L_1 \leqslant x \leqslant L, \tag{2}$$

where L_1 is the water depth and L is the total length of beam.

For free vibration of the beam, one has

$$y_1(x,t) = \bar{Y}_1(x)e^{i\bar{\omega}t}, \tag{3a}$$

$$y_2(x,t) = \bar{Y}_2(x)e^{i\bar{\omega}t}, \tag{3b}$$

where $\bar{Y}_1(x)$ and $\bar{Y}_2(x)$ denote the amplitude functions of $y_1(x,t)$ and $y_2(x,t)$, respectively, while $\bar{\omega}$ is the natural frequency of the (partially or fully) immersed beam and $i = \sqrt{-1}$.

The substitution of Eq. (3) into Eq. (1) gives

$$\bar{Y}_1''''(x) + \beta_w^4 \bar{Y}_1(x) = 0, \tag{4}$$

where

$$\beta_w^4 = \frac{(\rho + \rho_w)A}{EI}\,\bar{\omega}^2. \tag{5}$$

or

$$\bar{\omega} = (\beta_w L)^2 \sqrt{\frac{EI}{(\rho + \rho_w)AL^4}}. \tag{6}$$

The general solution of Eq. (4) takes the form [23]

$$\bar{Y}_1(x) = \bar{C}_1 \sin \beta_w x + \bar{C}_2 \cos \beta_w x + \bar{C}_3 \sinh \beta_w x + \bar{C}_4 \cosh \beta_w x. \tag{7}$$

Similarly, the mode shape of the emerged part of the beam takes the form

$$\bar{Y}_2(x) = \bar{C}_5 \sin \beta_a x + \bar{C}_6 \cos \beta_a x + \bar{C}_7 \sinh \beta_a x + \bar{C}_8 \cosh \beta_a x, \tag{8}$$

where

$$\beta_a^4 = \frac{\rho A}{EI}\,\bar{\omega}^2. \tag{9}$$

It is noted that the subscripts w and a for the parameters β_w and β_a, respectively, defined by Eqs. (5) and (9) are used to indicate that the parameter β_w is obtained based on the equivalent mass density of the beam in "water", $\rho + \rho_w$, while the parameter β_a is obtained based on the actual mass density of the beam in "air", ρ. In other words, corresponding to each natural frequency $\bar{\omega}$, one may obtain two frequency parameters, β_w and β_a. Disagreement between numerical results may be due to selecting wrong parameters for comparison as one may see from the section of "Numerical results and discussions" in this paper.

The eight integration constants, $\bar{C}_1 - \bar{C}_8$, appearing in Eqs. (7) and (8), are determined by the following boundary conditions:

$$EI\,\bar{Y}_1''(x) = k_R\,\bar{Y}_1'(x) \quad \text{at } x = 0, \tag{10a}$$

$$EI\,\bar{Y}_1'''(x) = -k_T\,\bar{Y}_1(x) \quad \text{at } x = 0, \tag{10b}$$

$$\bar{Y}_1(x) = \bar{Y}_2(x), \quad \bar{Y}_1'(x) = \bar{Y}_2'(x), \quad \bar{Y}_1''(x) = \bar{Y}_2''(x), \quad \bar{Y}_1'''(x) = \bar{Y}_2'''(x) \quad \text{at } x = L_1, \tag{11a,b,c,d}$$

$$EI\,\bar{Y}_2''(x) = \bar{\omega}^2(J_t + m_t e^2)\bar{Y}_2'(x) + \bar{\omega}^2 m_t e\,\bar{Y}_2(x) \quad \text{at } x = L, \tag{12a}$$

$$EI\,\bar{Y}_2'''(x) = -\bar{\omega}^2 m_t\,\bar{Y}_2(x) - \bar{\omega}^2 m_t e\,\bar{Y}_2'(x) \quad \text{at } x = L. \tag{12b}$$

It is noted that the boundary conditions given by Eqs. (10) and (11) are the classical ones because they are independent of the natural frequency $\bar{\omega}$. However, this is not true for those given by Eqs. (12a) and (12b), because they are frequency dependent. One of the main differences between this paper and Refs. [7,20] is due to the frequency-dependent boundary conditions.

Substituting Eq. (7) into Eqs. (10a) and (10b), one obtains

$$k_R\bar{C}_1 + EI\beta_w\bar{C}_2 + k_R\bar{C}_3 - EI\beta_w\bar{C}_4 = 0, \tag{13a}$$

$$EI\beta_w^3\bar{C}_1 - k_T\bar{C}_2 - EI\beta_w^3\bar{C}_3 - k_T\bar{C}_4 = 0. \tag{13b}$$

Similarly, the substitution of Eqs. (7) and (8) into Eqs. (11a)–(11d) leads to

$$\begin{aligned}&\sin\beta_w L_1\bar{C}_1 + \cos\beta_w L_1\bar{C}_2 + \sinh\beta_w L_1\bar{C}_3 + \cosh\beta_w L_1\bar{C}_4\\ &\quad - \sin\beta_a L_1\bar{C}_5 - \cos\beta_a L_1\bar{C}_6 - \sinh\beta_a L_1\bar{C}_7 - \cosh\beta_a L_1\bar{C}_8 = 0,\end{aligned} \tag{14a}$$

$$\begin{aligned}&\beta_w(\cos\beta_w L_1\bar{C}_1 - \sin\beta_w L_1\bar{C}_2 + \cosh\beta_w L_1\bar{C}_3 + \sinh\beta_w L_1\bar{C}_4)\\ &\quad + \beta_a(-\cos\beta_a L_1\bar{C}_5 + \sin\beta_a L_1\bar{C}_6 - \cosh\beta_a L_1\bar{C}_7 - \sinh\beta_a L_1\bar{C}_8) = 0,\end{aligned} \tag{14b}$$

$$\begin{aligned}&\beta_w^2(-\sin\beta_w L_1\bar{C}_1 - \cos\beta_w L_1\bar{C}_2 + \sinh\beta_w L_1\bar{C}_3 + \cosh\beta_w L_1\bar{C}_4)\\ &\quad + \beta_a^2(\sin\beta_a L_1\bar{C}_5 + \cos\beta_a L_1\bar{C}_6 - \sinh\beta_a L_1\bar{C}_7 - \cosh\beta_a L_1\bar{C}_8) = 0,\end{aligned} \tag{14c}$$

$$\begin{aligned}&\beta_w^3(-\cos\beta_w L_1\bar{C}_1 + \sin\beta_w L_1\bar{C}_2 + \cosh\beta_w L_1\bar{C}_3 + \sinh\beta_w L_1\bar{C}_4)\\ &\quad + \beta_a^3(\cos\beta_a L_1\bar{C}_5 - \sin\beta_a L_1\bar{C}_6 - \cosh\beta_a L_1\bar{C}_7 - \sinh\beta_a L_1\bar{C}_8) = 0.\end{aligned} \tag{14d}$$

Finally, from Eqs. (8) and (12), one obtains

$$\begin{aligned}&[-(EI\beta_a^2 + \bar{\omega}^2 m_t e)\sin\beta_a L - \bar{\omega}^2\beta_a(J_t + m_t e^2)\cos\beta_a L]\bar{C}_5\\ &\quad + [-(EI\beta_a^2 + \bar{\omega}^2 m_t e)\cos\beta_a L + \bar{\omega}^2\beta_a(J_t + m_t e^2)\sin\beta_a L]\bar{C}_6\\ &\quad + [(EI\beta_a^2 - \bar{\omega}^2 m_t e)\sinh\beta_a L - \bar{\omega}^2\beta_a(J_t + m_t e^2)\cosh\beta_a L]\bar{C}_7\\ &\quad + [(EI\beta_a^2 - \bar{\omega}^2 m_t e)\cosh\beta_a L - \bar{\omega}^2\beta_a(J_t + m_t e^2)\sinh\beta_a L]\bar{C}_8 = 0,\end{aligned} \tag{15a}$$

$$
\begin{aligned}
&[(-EI\beta_a^3+\bar{\omega}^2\beta_a m_t e)\cos\beta_a L+\bar{\omega}^2 m_t\sin\beta_a L]\bar{C}_5\\
&\quad+[(EI\beta_a^3-\bar{\omega}^2\beta_a m_t e)\sin\beta_a L+\bar{\omega}^2 m_t\cos\beta_a L]\bar{C}_6\\
&\quad+[(EI\beta_a^3+\bar{\omega}^2\beta_a m_t e)\cosh\beta_a L+\bar{\omega}^2 m_t\sinh\beta_a L]\bar{C}_7\\
&\quad+[(EI\beta_a^3+\bar{\omega}^2\beta_a m_t e)\sinh\beta_a L+\bar{\omega}^2 m_t\cosh\beta_a L]\bar{C}_8=0. \qquad (15b)
\end{aligned}
$$

To write Eqs. (13)–(15) in matrix form, one has

$$
\begin{bmatrix}
\bar{B}_{11} & \bar{B}_{12} & \bar{B}_{13} & \bar{B}_{14} & \bar{B}_{15} & \bar{B}_{16} & \bar{B}_{17} & \bar{B}_{18}\\
\bar{B}_{21} & \bar{B}_{22} & \bar{B}_{23} & \bar{B}_{24} & \bar{B}_{25} & \bar{B}_{26} & \bar{B}_{27} & \bar{B}_{28}\\
\bar{B}_{31} & \bar{B}_{32} & \bar{B}_{33} & \bar{B}_{34} & \bar{B}_{35} & \bar{B}_{36} & \bar{B}_{37} & \bar{B}_{38}\\
\bar{B}_{41} & \bar{B}_{42} & \bar{B}_{43} & \bar{B}_{44} & \bar{B}_{45} & \bar{B}_{46} & \bar{B}_{47} & \bar{B}_{48}\\
\bar{B}_{51} & \bar{B}_{52} & \bar{B}_{53} & \bar{B}_{54} & \bar{B}_{55} & \bar{B}_{56} & \bar{B}_{57} & \bar{B}_{58}\\
\bar{B}_{61} & \bar{B}_{62} & \bar{B}_{63} & \bar{B}_{64} & \bar{B}_{65} & \bar{B}_{66} & \bar{B}_{67} & \bar{B}_{68}\\
\bar{B}_{71} & \bar{B}_{72} & \bar{B}_{73} & \bar{B}_{74} & \bar{B}_{75} & \bar{B}_{76} & \bar{B}_{77} & \bar{B}_{78}\\
\bar{B}_{81} & \bar{B}_{82} & \bar{B}_{83} & \bar{B}_{84} & \bar{B}_{85} & \bar{B}_{86} & \bar{B}_{87} & \bar{B}_{88}
\end{bmatrix}
\begin{Bmatrix}
\bar{C}_1\\ \bar{C}_2\\ \bar{C}_3\\ \bar{C}_4\\ \bar{C}_5\\ \bar{C}_6\\ \bar{C}_7\\ \bar{C}_8
\end{Bmatrix}=0 \qquad (16)
$$

or

$$
[\bar{B}]\{\bar{C}\}=0, \qquad (17)
$$

where $\{\bar{C}\}$ is a column vector given by

$$
\{\bar{C}\}=\{\bar{C}_1\quad \bar{C}_2\quad \bar{C}_3\quad \bar{C}_4\quad \bar{C}_5\quad \bar{C}_6\quad \bar{C}_7\quad \bar{C}_8\} \qquad (18)
$$

and $[\bar{B}]$ is a 8×8 square matrix with its coefficients given by

$$
\bar{B}_{11}=k_R,\quad \bar{B}_{12}=EI\beta_w,\quad \bar{B}_{13}=k_R,\quad \bar{B}_{14}=-EI\beta_w,\quad \bar{B}_{1j}=0\quad (j=5-8), \qquad (19)
$$

$$
\bar{B}_{21}=EI\beta_w^3,\quad \bar{B}_{22}=-k_T,\quad \bar{B}_{23}=-EI\beta_w^3,\quad \bar{B}_{24}=-k_T,\quad \bar{B}_{2j}=0\quad (j=5-8), \qquad (20)
$$

$$
\begin{aligned}
&\bar{B}_{31}=\sin\beta_w L_1,\quad \bar{B}_{32}=\cos\beta_w L_1,\quad \bar{B}_{33}=\sinh\beta_w L_1,\quad \bar{B}_{34}=\cosh\beta_w L_1,\\
&\bar{B}_{35}=-\sin\beta_a L_1,\quad \bar{B}_{36}=-\cos\beta_a L_1,\quad \bar{B}_{37}=-\sinh\beta_a L_1,\quad \bar{B}_{38}=-\cosh\beta_a L_1, \qquad (21)
\end{aligned}
$$

$$
\begin{aligned}
&\bar{B}_{41}=\beta_w\cos\beta_w L_1,\quad \bar{B}_{42}=-\beta_w\sin\beta_w L_1,\quad \bar{B}_{43}=\beta_w\cosh\beta_w L_1,\quad \bar{B}_{44}=\beta_w\sinh\beta_w L_1,\\
&\bar{B}_{45}=-\beta_a\cos\beta_a L_1,\quad \bar{B}_{46}=\beta_a\sin\beta_a L_1,\quad \bar{B}_{47}=-\beta_a\cosh\beta_a L_1,\quad \bar{B}_{48}=-\beta_a\sinh\beta_a L_1, \qquad (22)
\end{aligned}
$$

$$
\begin{aligned}
&\bar{B}_{51}=-\beta_w^2\sin\beta_w L_1,\quad \bar{B}_{52}=-\beta_w^2\cos\beta_w L_1,\quad \bar{B}_{53}=\beta_w^2\sinh\beta_w L_1,\quad \bar{B}_{54}=\beta_w^2\cosh\beta_w L_1,\\
&\bar{B}_{55}=\beta_a^2\sin\beta_a L_1,\quad \bar{B}_{56}=\beta_a^2\cos\beta_a L_1,\quad \bar{B}_{57}=-\beta_a^2\sinh\beta_a L_1,\quad \bar{B}_{58}=-\beta_a^2\cosh\beta_a L_1, \qquad (23)
\end{aligned}
$$

$$
\begin{aligned}
&\bar{B}_{61}=-\beta_w^3\cos\beta_w L_1,\quad \bar{B}_{62}=\beta_w^3\sin\beta_w L_1,\quad \bar{B}_{63}=\beta_w^3\cosh\beta_w L_1,\quad \bar{B}_{64}=\beta_w^3\sinh\beta_w L_1,\\
&\bar{B}_{65}=\beta_a^3\cos\beta_a L_1,\quad \bar{B}_{66}=-\beta_a^3\sin\beta_a L_1,\quad \bar{B}_{67}=-\beta_a^3\cosh\beta_a L_1,\quad \bar{B}_{68}=-\beta_a^3\sinh\beta_a L_1, \qquad (24)
\end{aligned}
$$

$$\begin{aligned}
&\bar{B}_{7j} = 0 \quad (j = 1-4),\\
&\bar{B}_{75} = -(EI\beta_a^2 + \bar{\omega}^2 m_t e)\sin\beta_a L - \bar{\omega}^2\beta_a(J_t + m_t e^2)\cos\beta_a L,\\
&\bar{B}_{76} = -(EI\beta_a^2 + \bar{\omega}^2 m_t e)\cos\beta_a L + \bar{\omega}^2\beta_a(J_t + m_t e^2)\sin\beta_a L,\\
&\bar{B}_{77} = (EI\beta_a^2 - \bar{\omega}^2 m_t e)\sinh\beta_a L - \bar{\omega}^2\beta_a(J_t + m_t e^2)\cosh\beta_a L,\\
&\bar{B}_{78} = (EI\beta_a^2 - \bar{\omega}^2 m_t e)\cosh\beta_a L - \bar{\omega}^2\beta_a(J_t + m_t e^2)\sinh\beta_a L,
\end{aligned} \tag{25}$$

$$\begin{aligned}
&\bar{B}_{8j} = 0 \quad (j = 1-4),\\
&\bar{B}_{85} = (-EI\beta_a^3 + \bar{\omega}^2\beta_a m_t e)\cos\beta_a L + \bar{\omega}^2 m_t \sin\beta_a L,\\
&\bar{B}_{86} = (EI\beta_a^3 - \bar{\omega}^2\beta_a m_t e)\sin\beta_a L + \bar{\omega}^2 m_t \cos\beta_a L,\\
&\bar{B}_{87} = (EI\beta_a^3 + \bar{\omega}^2\beta_a m_t e)\cosh\beta_a L + \bar{\omega}^2 m_t \sinh\beta_a L,\\
&\bar{B}_{88} = (EI\beta_a^3 + \bar{\omega}^2\beta_a m_t e)\sinh\beta_a L + \bar{\omega}^2 m_t \cosh\beta_a L.
\end{aligned} \tag{26}$$

Eq. (16) or (17) represents a simultaneous equations, non-trivial solution for the integration constants $\bar{C}_1 - \bar{C}_8$ requires that their coefficient determinant is equal to zero, i.e.,

$$\Delta(\bar{\omega}) = |\bar{B}| = 0. \tag{27}$$

Eq. (27) denotes the frequency equation for the elastically supported beam with eccentric tip mass m_t and mass moment of inertia J_t as shown in Fig. 1 from which one may determine the natural frequencies $\bar{\omega}_r$ $(r = 1, 2, 3, \ldots)$ together with the associated frequency parameters β_{wr} and β_{ar} defined by Eqs. (5) and (9). Besides, based on the last values of β_{wr} and β_{ar} one may determine the associated integration constants $\bar{C}_1 - \bar{C}_8$ from Eq. (16), and the substitution of the values of $\bar{C}_1 - \bar{C}_8$ into Eqs. (7) and (8) one may obtain the corresponding mode shapes $\bar{Y}_r(x)$. It is evident that $\bar{Y}_r(x)$ is a combination of $\bar{Y}_{1r}(x)$ and $\bar{Y}_{2r}(x)$. For the special cases, one has $\bar{Y}_r(x) = \bar{Y}_{1r}(x)$ if the beam is fully immersed and $\bar{Y}_r(x) = \bar{Y}_{2r}(x)$ if the beam is fully emerged.

The foregoing formulations are for the elastically supported beam. They are also available for the fixedly supported beam if the matrix coefficients $\bar{B}_{ij}$ $(i = 1-2$ and $j = 1-4)$ are replaced by

$$\bar{B}_{11} = 1, \quad \bar{B}_{12} = 0, \quad \bar{B}_{13} = 1, \quad \bar{B}_{14} = 0, \tag{28}$$

$$\bar{B}_{21} = 0, \quad \bar{B}_{22} = 1, \quad \bar{B}_{23} = 0, \quad \bar{B}_{24} = 1. \tag{29}$$

The last coefficients are obtained from substituting Eq. (7) into the following boundary conditions for a clamped beam at its lower end (cf. Fig. 1):

$$\bar{Y}_1'(x) = 0, \quad \bar{Y}_1(x) = 0. \tag{30a,b}$$

It is evident that one may obtain the analytical (exact) natural frequencies and mode shapes of both the elastically and fixedly supported immersed beams from the same formulation and computer program. This is one of the merits of the presented unified approach.

3. Natural frequencies and normal mode shapes of a "dry" beam

In addition to the classical analytical method introduced in the last section, the title problem can also be solved with the approximate PAM presented in this section. To this end, the "distributed" added mass along the immersed part of the beam is replaced by a number of "point" (concentrated) added masses so that the dynamical characteristics of an immersed (wet) beam may be predicted by a fully emerged (dry) beam carrying a number of point added masses. In general, for an immersed beam carrying a number of in-span lumped masses other than the point added masses along the beam (located at either the immersed or the emerged part), the last classical analytical method will suffer much difficulty, but this is not true for the PAM.

The first step of PAM is to determine the lowest several natural frequencies and the associated normal mode shapes of the "dry" beam analytically. Next, the mode superposition method is used to derive the equation of motion of the dry beam carrying a number of point masses (may be point added masses or the other in-span lumped masses) and then the associated eigenvalue problem is solved with the conventional numerical method. For this reason, the free vibration analysis of the "dry" beam is performed in this section.

It is similar to Eq. (4) that the characteristic equation for a dry beam is given by

$$Y''''(x) - \beta^4 Y(x) = 0 \tag{31}$$

with

$$\beta = \sqrt[4]{\frac{\rho A}{EI}\omega^2}, \tag{32}$$

where all symbols have the same meanings as the associated ones for the immersed (wet) beam.

The solution of Eq. (31) takes the form

$$Y(x) = C_1 \sin \beta x + C_2 \cos \beta x + C_3 \sinh \beta x + C_4 \cosh \beta x. \tag{33}$$

If the lower end of the dry beam is elastically supported as shown in Fig. 1, then the simultaneous equations for the integration constants $C_1 - C_4$ are given by

$$\begin{bmatrix} B_{11} & B_{12} & B_{13} & B_{14} \\ B_{21} & B_{22} & B_{23} & B_{24} \\ B_{31} & B_{32} & B_{33} & B_{34} \\ B_{41} & B_{42} & B_{43} & B_{44} \end{bmatrix} \begin{Bmatrix} C_1 \\ C_2 \\ C_3 \\ C_4 \end{Bmatrix} = 0. \tag{34}$$

In addition to the normal procedures of substituting Eq. (33) into the associated boundary conditions, such as those given by Eqs. (10) and (12), to arrive at Eq. (34), the last matrix equation may also be obtained directly from Eq. (16) by eliminating the 3–6 rows, the 5–8 columns in 1–2 rows and 1–4 columns in 7–8 rows from the 8×8 matrix $[\bar{B}]$. Thus,

$$B_{ij} = \bar{B}_{ij} \quad (i = 1 - 2 \quad \text{and} \quad j = 1 - 4), \tag{35}$$

$$B_{ij} = \bar{B}_{i+4,j+4} \quad (i = 3 - 4 \quad \text{and} \quad j = 1 - 4), \tag{36}$$

where the associated values of B_{ij} are given by Eqs. (19), (20), (25) and (26) with $\beta_w = \beta_a = \beta$. It is evident that the matrix coefficients B_{ij} appearing in Eq. (35) must be replaced by those given by Eqs. (28) and (29) if the lower end of the dry beam is clamped.

It is similar to Eq. (27) that the natural frequencies of the dry beam may be obtained from the following frequency equation:

$$\begin{vmatrix} B_{11} & B_{12} & B_{13} & B_{14} \\ B_{21} & B_{22} & B_{23} & B_{24} \\ B_{31} & B_{32} & B_{33} & B_{34} \\ B_{41} & B_{42} & B_{43} & B_{44} \end{vmatrix} = 0. \tag{37}$$

For a specified natural frequency ω_r (or parameter β_r) obtained from Eq. (37), one may obtain the corresponding integration constants $C_1 - C_4$ from Eq. (34) and, in turn, the "natural" mode shape $Y_r(x)$ of the dry beam from Eq. (33).

The orthogonal condition for the mode shapes of the current vibrating system is to take the form [23]

$$\begin{aligned} \delta_{rs} &= \int_0^L Y_r(x)\rho A\, Y_s(x)\,\mathrm{d}x + Y_r(L)m_t\, Y_s(L) + Y_r(L)2m_t e\, Y'_s(L) + Y'_r(L)(J_t + m_t e^2)\, Y'_s(L) \\ &= \begin{cases} \delta_{rr} & \text{if } r = s, \\ 0 & \text{if } r \neq s. \end{cases} \end{aligned} \tag{38}$$

It is noted that the orthogonal condition given by Ref. [23] is only a simple general form and is not like that of Eq. (38). If each term on the right side of Eq. (38) is multiplied by the square of the rth natural frequency of the dry beam, ω_r^2, then the first term of the resulting expression denotes the work done by the inertia forces of the dry beam itself and all the other terms denote the works done by the frequency-dependent boundary forces and moments.

The mode superposition method is available only for the orthogonal "normal" mode shapes, the latter may be obtained from the "natural" mode shapes by using the normalization factor δ_{rr} determined by Eq. (38), i.e.,

$$\begin{aligned} \hat{Y}_r(x) &= Y_r(x)/\sqrt{\delta_{rr}} = \frac{1}{\sqrt{\delta_{rr}}}(C_1 \sin \beta_r x + C_2 \cos \beta_r x + C_3 \sinh \beta_r x + C_4 \cosh \beta_r x) \\ r &= 1, 2, 3, \ldots. \end{aligned} \tag{39}$$

For a general vibrating system with its boundary conditions independent upon its natural frequencies, such as those in Refs. [7,20], the normalization factor δ_{rr} is determined by the first term on the right-hand side of Eq. (38), i.e.,

$$\delta_{rr} = \int_0^L Y_r(x)\rho A\, Y_r(x)\,\mathrm{d}x. \tag{40}$$

However, this is incorrect for the current problem, because the boundary conditions at the top end of the beam are dependent on the natural frequencies as one may see from Eqs. (12a) and (12b).

4. Mathematical model for FEM and PAM

In order to determine the natural frequencies and mode shapes of the immersed beam with the conventional FEM, the whole beam shown in Fig. 1 is subdivided into N_e identical beam elements bound by $N_e + 1$ nodes. The last nodes are used as the P stations for the PAM, at which the point added masses $\tilde{m}_i$ ($i = 1$ to f) or in-span lumped mass m_i ($i = 2$ to $(P-1)$) are located as shown in Fig. 2, with f denoting the numbering for the station located at the free water surface. Since the sizes of all beam elements are identical, the total stations $P = N_e + 1$ are uniformly distributed over the whole length L of the beam with first station 1 at the lower end and the final station P at the upper end of the beam. In Fig. 2, the location of station i is defined by the coordinate x_i ($i = 1$ to P) with its origin at the first station, thus, one has $x_f = L_1$, where L_1 is the depth of water. According to the foregoing descriptions one sees that the magnitude of the concentrated mass at station i is determined by

$$\hat{m}_i = \tilde{m}_i + m_i \quad (i = 1 \text{ to } P), \tag{41}$$

where the magnitudes of the point added masses are given by [20]

$$\tilde{m}_i = C'_m \rho_w A L_1/(f-1) \quad \text{for } i = 2, 3, \ldots, f-1, \tag{42a}$$

$$\tilde{m}_i = \tfrac{1}{2} C'_m \rho_w A L_1/(f-1) \quad \text{for } i = 1 \text{ and } f. \tag{42b}$$

In the last expressions, C'_m is the added mass coefficient [24], and for simplicity, it is usually assumed that $C'_m = 1.0$ [22,24].

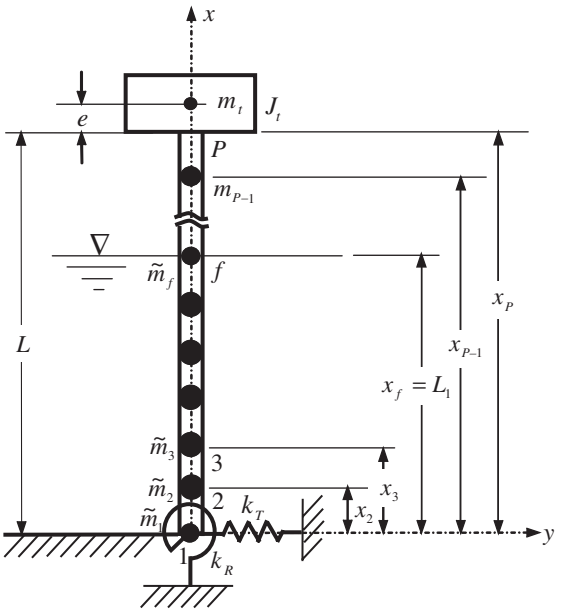

Fig. 2. Mathematical model for FEM and PAM (digits refer to the station numberings.)

Fig. 2 reveals that, for an immersed beam without any intermediate (in-span) point mass attached, one has $\hat{m}_i = \tilde{m}_i$ ($i = 1$ to f) for the immersed part and $\hat{m}_i = 0$ ($i = (f+1)$ to P) for the emerged part. Similarly, for an immersed beam with intermediate point masses attached, one has $\hat{m}_i = \tilde{m}_i + m_i$ ($i = 1$ to f) for the immersed part and $\hat{m}_i = m_i$ ($i = (f+1)$ to $(P-1)$) for the emerged part. In other words, Eq. (41) is correct for all possible cases shown in Fig. 2. At station i, if there exists no point "added mass" one has $\tilde{m}_i = 0$, if there exists no intermediate point mass one has $m_i = 0$ and if there exists neither point "added mass" nor intermediate point mass one has $\tilde{m}_i = m_i = 0$.

5. Point added mass method (PAM)

If the frequency-dependent boundary inertial forces and moments are neglected, then the equation of motion for a dry beam carrying P concentrated masses $\hat{m}_i$ ($i = 1$ to P), including the point added masses $\tilde{m}_i$ and the intermediate lumped masses m_i as shown in Fig. 2, is given by [7]

$$EIy''''(x,t) + \rho A\ddot{y}(x,t) + \sum_{i=1}^{P} \hat{m}_i \ddot{y}(x,t) \cdot \delta(x - x_i) = 0. \tag{43}$$

The definitions for the symbols appearing in Eq. (43) are exactly the same as those in Eq. (1) and $\delta(\cdot)$ denotes the Dirac delta function.

According to the theory of mode-superposition method [25], one may assume the dynamic response $y(x,t)$ satisfying Eq. (43) to take the form

$$y(x,t) = \sum_{s=1}^{n'} \hat{Y}_s(x) q_s(t), \tag{44}$$

where $\hat{Y}_s(x)$ denotes the sth normal mode shape of the dry beam given by Eq. (39), $q_s(t)$ is the sth generalized coordinate, and n' is the total number of modes considered.

Substituting Eq. (44) into Eq. (43), pre-multiplying both sides of the resulting equation by $\hat{Y}_r(x)\,\mathrm{d}x$, integrating each term over the beam length ($x = 0$ to L), considering the influence of frequency-dependent boundary inertial forces and moments, and applying the orthogonal condition given by Eq. (38), one obtains

$$\hat{M}_{rr}\ddot{q}_r(t) + \hat{K}_{rr} q_r(t) = \hat{P}_r(t) \quad (r = 1 - n'), \tag{45}$$

where

$$\hat{M}_{rr} = \int_0^L \hat{Y}_r(x)\rho A\,\hat{Y}_r(x)\,\mathrm{d}x + \hat{Y}_r(L) m_t\,\hat{Y}_r(L) + 2m_t e\,\hat{Y}_r(L)\,\hat{Y}'_r(L) + \hat{Y}'_r(L)(J_t + m_t e^2)\,\hat{Y}'_r(L), \tag{46a}$$

$$\hat{K}_{rr} = \int_0^L \hat{Y}_r(x) EI\,\hat{Y}''''_{rr}(x)\,\mathrm{d}x, \tag{46b}$$

$$\hat{P}_r = -\left[\sum_{i=1}^{p}\sum_{s=1}^{n'} \hat{m}_i\,\hat{Y}_r(x_i)\,\hat{Y}_s(x_i)\right]\ddot{q}_r(t) \tag{46c}$$

represent the generalized mass, generalized stiffness and generalized force, respectively. For the "normal" mode shapes $\hat{Y}_r(x)$ given by Eq. (39), one has

$$\hat{M}_{rr} = 1.0 \quad \text{and} \quad \hat{K}_{rr}/\hat{M}_{rr} = \omega_r^2, \tag{47a,b}$$

where ω_r represents the rth natural frequency of the dry beam.

Eq. (45) is the governing equation for the wet beam. When the wet beam performs free vibration, the generalized coordinate $q_r(t)$ in Eq. (45) takes the form

$$q_r(t) = \bar{q}_r e^{i\tilde{\omega}t}, \tag{48}$$

where $\bar{q}_r$ is the amplitude of $q_r(t)$ and $\tilde{\omega}$ is the natural frequency of the wet beam.

From Eqs. (45)–(48) one obtains

$$(\omega_r^2 - \tilde{\omega}^2)\bar{q}_r - \tilde{\omega}^2\left(\sum_{i=1}^{P}\sum_{s=1}^{n'} m_i \hat{Y}_r(x_i)\hat{Y}_s(x_i)\right)\bar{q}_r = 0, \quad r = 1\sim n' \tag{49}$$

or in matrix form

$$\left[\omega^2\right]\{\bar{q}\} - \tilde{\omega}^2\left(\left[I\right] + [A]\right)\{\bar{q}\} = 0, \tag{50}$$

where

$$\begin{aligned} \{\hat{Y}(x)\} &= \{\hat{Y}_1(x), \hat{Y}_2(x), \ldots, \hat{Y}_{n'}(x)\}_{n'\times 1}, \quad \{\bar{q}\} = \{\bar{q}_1, \bar{q}_2, \ldots, \bar{q}_{n'}\}_{n'\times 1}, \\ \left[\omega^2\right] &= \lceil \omega_1^2, \omega_2^2, \ldots, \omega_{n'}^2 \rfloor_{n'\times n'}, \quad \left[I\right] = \lceil 1, 1, \ldots, 1 \rfloor_{n'\times n'}, \\ [A] &= \sum_{i=1}^{P} m_i \{\hat{Y}(x_i)\}\{\hat{Y}(x_i)\}^{\mathrm{T}}. \end{aligned} \tag{51}$$

In the above expressions, the symbols $\{\}$, $\lceil\ \rfloor$ and $[\,]$ represent a column matrix, a diagonal matrix and a square matrix, respectively.

Eq. (50) is an eigenvalue equation, a lot of techniques [26] may be used to obtain the eigenvalues $\tilde{\omega}_r$ $(r = 1, \ldots, n')$ and the corresponding eigenvectors $\{\bar{q}\}_r$ $(r = 1, \ldots, n')$. Here $\tilde{\omega}_r$ is the rth natural frequency of the "wet "beam with the corresponding mode shape $\tilde{Y}_r(x)$ determined by

$$\tilde{Y}_r(x) = \sum_{s=1}^{n'} \hat{Y}_s(x)\{\bar{q}\}_s. \tag{52}$$

The last formulation of PAM is extended from that of the unified approach without any difficulty, this is another merit of the presented unified approach.

6. Numerical results and discussions

For comparison, the main dimensions and physical properties of the beam are taken to be equal to those of Refs. [13,19]: total length $L = 15\,\mathrm{m}$, diameter $d = 0.3\,\mathrm{m}$, cross-sectional area $A = \pi d^2/4 = 7.06858 \times 10^{-2}\,\mathrm{m}^2$, moment of inertia of cross-sectional area $I = \pi d^4/64 = 3.9761 \times 10^{-4}\,\mathrm{m}^4$, Young's modulus $E = 2.068 \times 10^{11}\,\mathrm{N/m}^2$ and mass density of

beam material $\rho = 7850\,\mathrm{kg/m^3}$. Besides, the mass density of water and added mass coefficient are taken to be $\rho_w = 1000\,\mathrm{kg/m^3}$ and $C'_m = 1.0$, respectively. For convenience, the following non-dimensional parameters are introduced: draft ratio $L_1^* = L_1/L = L_1/15$, rotary-inertia ratio $J_t^* = J_t/(\rho A L^3) = J_t/(1.87273191375 \times 10^6)$, tip-mass ratio $m_t^* = m_t/(\rho A L) = m_t/(8.32325295 \times 10^3)$, translational spring stiffness ratio $k_t^* = k_t/(EI/L^3) = k_t/(2.43631846 \times 10^4)$ and rotational spring stiffness ratio $k_R^* = k_R/(EI/L) = k_R/(5.4817165333 \times 10^6)$. Unless particularly stated, the results of this paper are obtained based on the following values of parameters: eccentricity $e = 0.5\,\mathrm{m}$, rotary-inertia ratio $J_t^* = 0.1$, tip-mass ratio $m_t^* = 0.1$, total number of finite beam elements $N_e = 60$, total number of stations $P = N_e + 1 = 61$.

6.1. Reliability of the theory and the computer programs

In order to confirm the reliability of the theory and the computer programs developed for this paper, the influence of rotary-inertia ratio J_t^*, draft ratio L_1^* and tip-mass ratio m_t^* on the lowest three frequency parameters of the "fixed" immersed beam with zero eccentricity (i.e., $e = 0$), $(\beta_w L)_r$ and $(\beta_a L)_r$ for $r = 1 - 3$, are studied and shown in Table 1. It has been mentioned next to Eq. (9) that corresponding to each natural frequency $\bar{\omega}$, one may obtain two frequency parameters, β_w and β_a, from Eqs. (5) and (9), respectively. However, in Ref. [13] only the parameter β_w is calculated, and in Ref. [19] only the parameter β_a is calculated. This is the reason why, in Table 2 of Ref. [13], the frequency parameters of Ref. [13] are different from the corresponding ones of Ref. [19] to some degree. From the current Table 1 one sees that the frequency parameters obtained from this paper (either Exact, PAM or FEM) are very close to the corresponding ones of Refs. [13,19]. In other words, all the frequency parameters listed in Table 2 of Ref. [13] are correct. It seems that the author of Ref. [14] does not find the last fact yet. It is noted that the natural frequencies of the immersed beam, $\bar{\omega}_r$ $(r = 1, 2, 3, \ldots)$, obtained from either Ref. [13] or [14] should be very close to the corresponding ones of Ref. [19], because both β_w and β_a are determined from the same associated natural frequency $\bar{\omega}_r$ as one may see from Eqs. (5) and (9).

It is believed that the above-mentioned good agreement between the natural frequencies of this paper and the corresponding ones of the existing literature may be the evidence of reliability of the theory and the computer programs developed for this paper.

6.2. Influence of spring stiffness ($k_T = k_R$) of the elastically supported immersed beam

In this paper, the analytical solutions of natural frequencies and mode shapes for both the elastically and fixedly supported immersed beams are presented. The main purpose of this subsection is to show that natural frequencies and mode shapes of a fixedly supported (clamped) immersed beam may also be obtained from the elastically supported one by simply setting the stiffness of the elastic-support springs to approach infinity.

For the case of $e = 0.5\,\mathrm{m}$ and $J_t^* = m_t^* = 0.1$, the influence of the stiffness ratios $k_T^* = k_R^*$ on the lowest five natural frequencies of the immersed beam is shown in Table 2 with draft ratios $L_1^* = L_1/L = 0$, 0.5 and 1.0, respectively, where "Exact" refers to the analytical (exact) method and "PAM" refers to the point added mass method, both of them are presented in this paper. For the case of $k_T^* = k_R^* = \infty$ as shown in Table 2, the associated lowest five natural frequencies are

Table 1
Influence of draft ratios ($L_1^* = L_1/L$), rotary-inertia ratios ($J_t^* = J_t/(\rho AL^3)$) and tip-mass ratios ($m_t^* = m_t/(\rho AL)$) on the lowest three frequency parameters of the "fixed" immersed beam with eccentricity $e = 0$ shown in Fig. 1, $(\beta_w L)_r$ and $(\beta_a L)_r$ for $r = 1 - 3$

J_t^*	L_1^*	m_t^*	Methods	$(\beta_w L)_1$	$(\beta_w L)_2$	$(\beta_w L)_3$	$(\beta_a L)_1$	$(\beta_a L)_2$	$(\beta_a L)_3$
0.0	0.0	1.0	Ref. [13]	1.28589	4.15381	7.35123	—	—	—
			Ref. [19]	—	—	—	1.24791	4.03105	7.13373
			Exact	1.28589	4.15381	7.35122	1.24792	4.03114	7.13413
			PAM	1.28589	4.15381	7.35122	1.24792	4.03114	7.13413
			FEM	1.28589	4.15381	7.35122	1.24792	4.03114	7.13413
		2.0	Ref. [13]	1.10894	4.10377	7.31879	—	—	—
			Ref. [19]	—	—	—	1.07619	3.98250	7.10227
			Exact	1.10894	4.10376	7.31878	1.07619	3.98257	7.10265
			PAM	1.10894	4.10376	7.31878	1.07619	3.98257	7.10265
			FEM	1.10894	4.10376	7.31878	1.07620	3.98257	7.10265
	0.5	1.0	Ref. [13]	1.28553	4.10890	7.23281	—	—	—
			Ref. [19]	—	—	—	1.24755	3.98642	7.01864
			Exact	1.28553	4.10890	7.23280	1.24757	3.98756	7.01921
			PAM	1.28553	4.10889	7.23284	1.24757	3.98755	7.01925
			FEM	1.28553	4.10889	7.23284	1.24757	3.98755	7.01925
		2.0	Ref. [13]	1.10878	4.05978	7.20006	—	—	—
			Ref. [19]	—	—	—	1.07602	3.93877	6.98687
			Exact	1.10877	4.05978	7.20006	1.07603	3.93989	6.98743
			PAM	1.10877	4.05977	7.20010	1.07603	3.93988	6.98747
			FEM	1.10878	4.05977	7.20010	1.07603	3.93988	6.98747
1.0	0.0	1.0	Ref. [13]	0.95996	1.89739	5.05001	—	—	—
			Ref. [19]	—	—	—	0.93161	1.84135	4.90076
			Exact	0.95996	1.89738	5.05001	0.93161	1.84135	4.90087
			PAM	0.95996	1.89738	5.05001	0.93161	1.84135	4.90087
			FEM	0.95996	1.89738	5.05001	0.93161	1.84135	4.90087
		2.0	Ref. [13]	0.91265	1.74078	4.97632	—	—	—
			Ref. [19]	—	—	—	0.78792	1.59862	4.82488
			Exact	0.91265	1.74078	4.97631	0.88570	1.68937	4.82936
			PAM	0.91265	1.74078	4.97631	0.88570	1.68937	4.82936
			FEM	0.91265	1.74078	4.97631	0.88570	1.68937	4.82936
	0.5	1.0	Ref. [13]	0.95991	1.98600	4.97223	—	—	—
			Ref. [19]	—	—	—	0.93156	1.83996	4.82388
			Exact	0.95991	1.89600	4.97223	0.93156	1.84001	4.82539
			PAM	0.95991	1.89600	4.97224	0.93156	1.84001	4.82540
			FEM	0.95991	1.89600	4.97224	0.93156	1.84001	4.82540
		2.0	Ref. [13]	0.91261	1.74004	4.89985	—	—	—
			Ref. [19]	—	—	—	0.78789	1.59794	4.74919
			Exact	0.91260	1.74004	4.89984	0.88565	1.68865	4.75514
			PAM	0.91260	1.74004	4.89985	0.88565	1.68865	4.75515
			FEM	0.91261	1.74004	4.89985	0.88565	1.68866	4.75515

Note: $\beta_w = \sqrt[4]{\frac{(\rho+\rho_w)A}{EI}\bar{\omega}^2}$, $\beta_a = \sqrt[4]{\frac{\rho A}{EI}\bar{\omega}^2}$.

Table 2
Influence of spring-stiffness ratios ($k_T^* = k_R^*$) on the lowest five natural frequencies of the elastically supported immersed beam with eccentricity $e = 0.5$ m and $J_t^* = m_t^* = 0.1$ for the cases of draft ratios $L_1^* = L_1/L = 0$, 0.5, 1.0

Draft ratios $L_1^* = L_1/L$	Stiffness ratios $k_T^* = k_R^*$ [a]	Methods	Natural frequencies, $\bar{\omega}_r$ (or $\tilde{\omega}_r$) (rad/s)				
			$\bar{\omega}_1$ (or $\tilde{\omega}_1$)[b]	$\bar{\omega}_2$ (or $\tilde{\omega}_2$)	$\bar{\omega}_3$ (or $\tilde{\omega}_3$)	$\bar{\omega}_4$ (or $\tilde{\omega}_4$)	$\bar{\omega}_5$ (or $\tilde{\omega}_5$)
0.0	1	Exact	1.35248	3.46108	14.31519	51.59763	122.83709
		PAM	1.35219	3.45871	14.29530	51.49903	122.59260
	10^2	Exact	3.77178	10.47159	30.21314	68.10286	143.72022
		PAM	3.77178	10.47120	30.18476	68.01004	143.54379
	10^4	Exact	3.85262	11.66778	48.63279	118.12376	217.54473
		PAM	3.85262	11.66778	48.63277	118.12289	217.53306
	10^8	Exact	3.85344	11.68087	48.90630	119.83452	223.90719
		PAM	3.85344	11.68087	48.90630	119.83452	223.90719
	10^{16}	Exact	3.85344	11.68088	48.90633	119.83469	223.90777
		PAM	3.85344	11.68088	48.90633	119.83469	223.90777
	∞ (Fixed)	Exact	3.85344	11.68088	48.90633	119.83469	223.90777
0.5	1	Exact	1.32839	3.39042	13.96936	49.91881	119.48084
		PAM	1.32839	3.39041	13.96915	49.91681	119.47037
	10^2	Exact	3.76692	10.38251	28.86645	65.96007	139.37345
		PAM	3.76691	10.38249	28.86666	65.95963	139.37369
	10^4	Exact	3.84893	11.61686	47.08529	114.87197	210.50292
		PAM	3.84892	11.61682	47.08579	114.87030	210.51032
	10^8	Exact	3.84975	11.63030	47.36448	116.60221	217.03449
		PAM	3.84975	11.63025	47.36498	116.60058	217.04141
	10^{16}	Exact	3.84975	11.63030	47.36451	116.60237	217.03508
		PAM	3.84975	11.63026	47.36501	116.60075	217.04200
	∞ (Fixed)	Exact	3.84975	11.63030	47.36451	116.60237	217.03508
1.0	1	Exact	1.28692	3.37885	13.80770	48.98336	116.32190
		PAM	1.28691	3.37882	13.80756	48.98130	116.31352
	10^2	Exact	3.68100	10.17484	28.63831	64.53880	136.03870
		PAM	3.68097	10.17488	28.63836	64.53883	136.03866
	10^4	Exact	3.76541	11.35052	46.17898	111.86042	205.73221
		PAM	3.76538	11.35057	46.17909	111.86070	205.73326
	10^8	Exact	3.76627	11.36336	46.44080	113.49083	211.78095
		PAM	3.76624	11.36340	46.44090	113.49107	211.78188
	10^{16}	Exact	3.76627	11.36336	46.44083	113.49099	211.78150
		PAM	3.76624	11.36341	46.44093	113.49123	211.78243
	∞(Fixed)	Exact	3.76627	11.36336	46.44083	113.49099	211.78150

[a] $k_t^* = k_t/(EI/L^3)$, $k_R^* = k_R/(EI/L)$.
[b] $\bar{\omega}_r$ and $\tilde{\omega}_r$ denote the rth natural frequencies obtained from Exact method and PAM, respectively.

the "exact" values obtained from the formulation of fixedly supported immersed beam with boundary conditions defined by Eqs. (30a,b) rather than the "approximate" ones obtained from the elastically supported beam by setting $k_T^* = k_R^* = \infty$.

From Table 2 one sees the following: (i) the natural frequencies obtained from the PAM (denoted by $\tilde{\omega}_r$) are very close to the corresponding ones obtained from the Exact method

(denoted by $\bar{\omega}_r$). (ii) The natural frequencies of the elastically supported immersed beam obtained either from PAM or Exact method converge to the corresponding ones of the fixedly supported beam when $k_T^* = k_R^* = 10^{16}$. (iii) The natural frequencies (accurate to the 5th decimal place) of the elastically supported immersed beam obtained from the Exact method are exactly equal to the corresponding ones of the fixedly supported beam when $k_T^* = k_R^* = 10^{16}$, but this is not true for those obtained from PAM. (iv) The natural frequencies of the elastically supported immersed beam increase with increasing the stiffness ratios $k_T^* = k_R^*$. (v) For any specified stiffness ratios ($k_T^* = k_R^*$), the natural frequencies of the beam decrease with increasing the draft ratio $L_1^* = L_1/L$, but the effect of draft ratio is much smaller than that of the stiffness ratios.

For the case of $L_1^* = L_1/L = 0.5$ (or water depth $L_1 = 7.5$ m), the lowest five mode shapes of the elastically supported immersed beam (with $k_Y^* = k_R^* = 1$) and those of the fixedly supported one are shown in Figs. 3(a) and (b), respectively, where the dashed curves with symbols, ○, +, △, □ and ☆ denote the 1st, 2nd, 3rd, 4th and 5th mode shapes obtained from the Exact method, while the solid curves with ●, ×, ▲, ■ and ★ denote those obtained from the PAM. From the two figures one sees that the mode shapes obtained from the PAM are very close to the corresponding ones obtained from the Exact method. This is under one's expectation because the natural frequencies obtained from the last two methods are very close to each other as one may see from Table 2. Besides, from Fig. 3(a), one sees that the 1st and 2nd mode shapes of the elastically supported immersed beam are the modes major in the translational and rotational rigid-body motions, respectively, and the total numbers of "nodes" for the 3rd, 4th and 5th mode

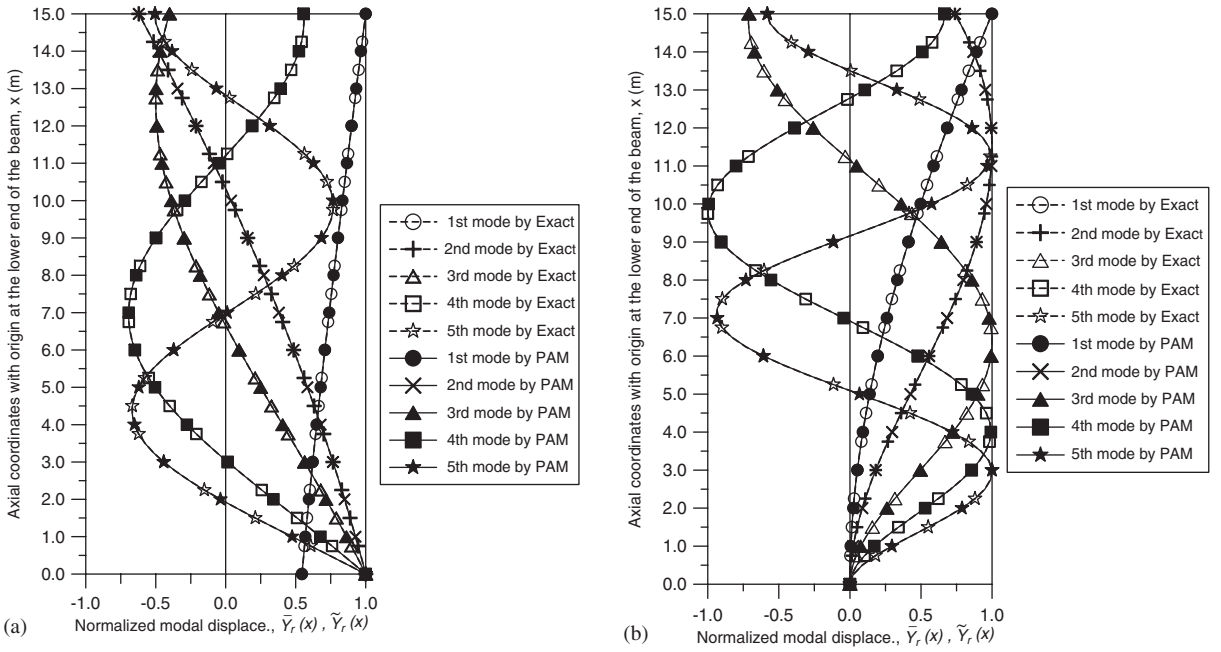

Fig. 3. The lowest five mode shapes of the elastically supported immersed beam with $L_1^* = L_1/L = 0.5$, $e = 0.5$ m and $J_t^* = m_t^* = 0.1$ obtained from the Exact method (------) and PAM (——) for: (a) $k_T^* = k_R^* = 1$; (b) $k_T^* = k_R^* = 10^{16}$ (or fixed supported).

shapes are 1, 2 and 3, respectively. On the other hand, from Fig. 3(b) one sees that all the five modes are the elastic vibration modes with total numbers of nodes being 0, 0, 1, 2, and 3, respectively. It is noted that the lower end of the beam is the supporting point and is not considered as a "node" for each mode shape. Although the 3rd, 4th and 5th mode shapes of either the elastically supported beam (cf. Fig. 3(a)) or those of the fixedly supported beam (cf. Fig. 3(b)) are the elastic vibration modes and the total numbers of "nodes" are also 1, 2 and 3, respectively, the profiles of the 3rd, 4th and 5th mode shapes for the elastically supported beam are much different from those for the fixedly supported beam as one may see from Figs. 3(a) and (b). This is also expected because the boundary conditions at the supporting (lower) end of the elastically supported beam are much different from those of the fixedly supported beam, the translational and rotational degrees of freedom (DOFs) for the latter are completely restrained and this is not true for the former.

6.3. Influence of eccentricity of tip mass

For the case of $J_t^* = m_t^* = 0.1$, the influence of eccentricity e (= 0, 0.5, 1.0 and 1.5 m) on the lowest five natural frequencies of the fixed beam is shown in Table 3 with draft ratios $L_1^* = L_1/L = 0$, 0.5 and 1.0, respectively. From Table 3 one sees that the first natural frequencies $\bar{\omega}_1$ decrease with increasing the eccentricity e, but this trend is reversed for the other four natural frequencies ($\bar{\omega}_2$ to $\bar{\omega}_5$). Besides, the effect of e decreases with increasing the draft ratio. The last phenomenon may be due to the fact that the total effective mass (m_{eff}) of the immersed beam increases with increasing the draft ratio so that the ratio of the tip mass m_t to total effective mass m_{eff} decreases with increasing the draft ratio. Besides, the effect of eccentricity e does not seem to be significant, this may be due to the small tip-mass ratio ($m_t^* = 0.1$) for the present example. From Table 3 one also sees that the natural frequencies obtained from PAM (denoted by $\tilde{\omega}_r$) are very close to those from the Exact method (denoted by $\bar{\omega}_r$).

6.4. Influence of tip-mass ratio and rotary-inertia ratio

According to Eq. (12), the effect of tip mass m_t is dependent on its eccentricity e and this is not true for the rotary inertia J_t, thus, one sets $e = 0$ in this subsection. For the case of rotary-inertia ratio $J_t^* = J_t/(\rho A L^3) = 0.1$, the influence of tip-mass ratios ($m_t^* = 1$, 2, 3 and 4) on the lowest five natural frequencies of the fixed immersed beam is shown in Table 4 with draft ratios $L_1^* = L_1/L = 0$ and 1.0, respectively. Similarly, the influence of rotary-inertia ratios ($J_t^* = 1$, 2, 3 and 4) with $m_t^* = m_t/(\rho A L) = 0.1$ is shown in Table 5. In Table 4, the percentage differences ε_{r,m_t^*} are determined by the formula $\varepsilon_{r,m_t^*}\% = [(\bar{\omega}_r)_{m_t^*=1} - (\bar{\omega}_r)_{m_t^*}] \times 100\%/(\bar{\omega}_r)_{m_t^*=1}$ for $r = 1-5$ and $m_t^* = 2, 3, 4$. While in Table 5, the percentage differences ε_{r,J_t^*} are determined by $\varepsilon_{r,J_t^*}\% = [(\bar{\omega}_r)_{J_t^*=1} - (\bar{\omega}_r)_{J_t^*}] \times 100\%/(\bar{\omega}_r)_{J_t^*=1}$ for $r = 1-5$ and $J_t^* = 2, 3, 4$. In other words, from the value of ε_{r,m_t^*} (or ε_{r,J_t^*}) one may realize the reducing rate of the rth natural frequency $\bar{\omega}_r$ associated with the arbitrary tip-mass ratio m_t^* (or rotary-inertia ratio J_t^*) with respect to the value of $\bar{\omega}_r$ associated with $m_t^* = 1$ (or $J_t^* = 1$). It is evident that the larger the value of ε_{r,m_t^*} (or ε_{r,J_t^*}), the larger the effect of the tip-mass ratio m_t^* (or rotary-inertia ratio J_t^*).

The positive values of ε_r in Tables 4 and 5 indicate that increasing either the tip mass m_t or rotary inertia J_t will result in the decrease of the lowest five natural frequencies of the immersed

Table 3
Influence of tip-mass eccentricity e on the lowest five natural frequencies of the "fixed" immersed beam with $J_t^* = m_t^* = 0.1$ for the cases of draft ratios $L_1^* = L_1/L = 0$, 0.5, 1.0

Draft ratios $L_1^* = L_1/L$	Eccentricity of tip mass e (m)	Methods	Natural frequencies, $\bar{\omega}_r$ (or $\tilde{\omega}_r$) (rad/s)				
			$\bar{\omega}_1$ (or $\tilde{\omega}_1$)[a]	$\bar{\omega}_2$ (or $\tilde{\omega}_2$)	$\bar{\omega}_3$ (or $\tilde{\omega}_3$)	$\bar{\omega}_4$ (or $\tilde{\omega}_4$)	$\bar{\omega}_5$ (or $\tilde{\omega}_5$)
0.0	0	Exact	3.88979	11.62215	48.80593	119.73574	223.81344
		PAM	3.88979	11.62215	48.80593	119.73574	223.81344
	0.5	Exact	3.85344	11.68088	48.90633	119.83469	223.90777
		PAM	3.85344	11.68088	48.90633	119.83469	223.90777
	1.0	Exact	3.81619	11.73433	49.01003	119.94414	224.01868
		PAM	3.81619	11.73433	49.01003	119.94414	224.01868
	1.5	Exact	3.77814	11.78250	49.11646	120.06350	224.14562
		PAM	3.77814	11.78250	49.11646	120.06350	224.14562
0.5	0	Exact	3.88599	11.57271	47.26680	116.50361	216.94298
		PAM	3.88598	11.57268	47.26729	116.50199	216.94989
	0.5	Exact	3.84975	11.63030	47.36451	116.60237	217.03508
		PAM	3.84975	11.63026	47.36501	116.60075	217.04200
	1.0	Exact	3.81262	11.68262	47.46526	116.71136	217.14301
		PAM	3.81262	11.68257	47.46577	116.70973	217.14995
	1.5	Exact	3.77469	11.72966	47.56849	116.82997	217.26622
		PAM	3.77469	11.72962	47.56900	116.82833	217.27319
1.0	0	Exact	3.80007	11.31248	46.34526	113.39560	211.68967
		PAM	3.80004	11.31253	46.34536	113.39584	211.69058
	0.5	Exact	3.76627	11.36336	46.44083	113.49099	211.78150
		PAM	3.76624	11.36341	46.44093	113.49123	211.78243
	1.0	Exact	3.73159	11.40878	46.53894	113.59574	211.88859
		PAM	3.73157	11.40882	46.53905	113.59600	211.88955
	1.5	Exact	3.69614	11.44876	46.63906	113.70928	212.01037
		PAM	3.69611	11.44881	46.63917	113.70955	212.01136

[a] $\bar{\omega}_r$ and $\tilde{\omega}_r$ denote the rth natural frequencies obtained from Exact method and PAM, respectively.

beam. Besides, it is seen that: (i) the effect of m_t^* (or J_t^*) decreases with increasing the order (r) of vibration except the second mode ($r = 2$) of Table 4. (ii) The effect of J_t^* is greater than that of m_t^*. (iii) The influence of m_t^* on the first natural frequency ($r = 1$) is very significant and on the fifth one ($r = 5$) is very small. Although the influence of J_t^* on the first natural frequency ($r = 1$) is also very significant, that on the fourth and fifth ones ($r = 4$ and 5) is negligible.

6.5. Free vibration analysis of an immersed beam with in-span lumped masses

The immersed beam studied in this subsection is exactly the same as the one studied in Section 6.2, the only difference is that the current beam carries two identical intermediate (in-span) lumped masses at stations 53 and 57 (i.e., $x_{53} = 13\,\text{m}$ and $x_{57} = 14\,\text{m}$) with magnitudes $m_{53} = m_{57} = 0.5(\rho AL)\,\text{kg}$ and the beam in Section 6.2 does not carry any in-span point masses

Table 4
Influence of tip-mass ratio m_t^* on the lowest five natural frequencies of the "fixed" immersed beam with eccentricity $e = 0$ and rotary-inertia ratio $J_t^* = J_t/(\rho AL^3) = 0.1$ based on the Exact method for the cases of draft ratios $L_1^* = L_1/L = 0$, 1.0

Draft ratios $L_1^* = L_1/L$	Tip-mass ratios $m_t^* = m_t/(\rho AL)$	Natural frequencies, $\bar{\omega}_r$ (rad/s)				
		$\bar{\omega}_1$	$\bar{\omega}_2$	$\bar{\omega}_3$	$\bar{\omega}_4$	$\bar{\omega}_5$
0.0	1	2.44591	10.73632	42.34698	109.05790	210.24690
	2	1.88748	10.55226	41.23872	107.66600	208.76420
		(22.8312%)	(1.7144%)	(2.6171%)	(1.2763%)	(0.7052%)
	3	1.59225	10.47903	40.81467	107.16000	208.23840
		(34.9015%)	(2.3964%)	(3.6185%)	(1.7403%)	(0.9553%)
	4	1.40270	10.43972	40.59075	106.89840	207.96920
		(42.6512%)	(2.7626%)	(4.1472%)	(1.9801%)	(1.0833%)
1.0	1	2.42177	10.61239	40.28540	103.08400	198.38150
	2	1.87621	10.45681	39.16544	101.64390	196.83510
		(22.5273%)	(1.4660%)	(2.7801%)	(1.3970%)	(0.7795%)
	3	1.58545	10.39380	38.73033	101.11490	196.28260
		(34.5334%)	(2.0598%)	(3.8601%)	(1.9102%)	(1.0580%)
	4	1.39803	10.35971	38.49907	100.84020	195.99890
		(42.2724%)	(2.3810%)	(4.4342%)	(2.1766%)	(1.2010%)

$\varepsilon_{r,m_t^*}\% = [(\bar{\omega}_r)_{m_t^*=1} - (\bar{\omega}_r)_{m_t^*}] \times 100\%/(\bar{\omega}_r)_{m_t^*=1}$ for $r = 1-5$ and $m_t^* = 2, 3, 4$.

Table 5
Influence of rotary-inertia ratio J_t on the lowest five natural frequencies of the "fixed" immersed beam with eccentricity $e = 0$ and tip-mass ratio $m_t^* = m_t/(\rho AL) = 0.1$ based on the Exact method for the cases of draft ratios $L_1^* = L_1/L = 0$, 1.0

Draft ratios $L_1^* = L_1/L$	Tip-mass ratios $J_t^* = J_t/(\rho AL^3)$	Natural frequencies, $\bar{\omega}_r$ (rad/s)				
		$\bar{\omega}_1$	$\bar{\omega}_2$	$\bar{\omega}_3$	$\bar{\omega}_4$	$\bar{\omega}_5$
0.0	1	1.64802	8.85173	48.04049	119.40080	223.62270
	2	1.18731	8.69757	47.99856	119.38230	223.61210
		(27.9554%)	(1.7416%)	(0.0873%)	(0.0155%)	(0.0047%)
	3	0.97550	8.64665	47.98460	119.37610	223.60860
		(40.8078%)	(2.3168%)	(0.1163%)	(0.0207%)	(0.0063%)
	4	0.84745	8.62129	47.97762	119.37300	223.60690
		(48.5777%)	(2.6033%)	(0.1309%)	(0.0232%)	(0.0071%)
1.0	1	1.64278	8.45944	45.55385	113.04990	211.49240
	2	1.18541	8.29973	45.51056	113.03080	211.48150
		(27.8412%)	(1.8879%)	(0.0950%)	(0.0169%)	(0.0052%)
	3	0.97447	8.24702	45.49615	113.02440	211.47790
		(40.6816%)	(2.5110%)	(0.1267%)	(0.0225%)	(0.0069%)
	4	0.84678	8.22078	45.48895	113.02120	211.47600
		(48.4544%)	(2.8212%)	(0.1425%)	(0.0253%)	(0.0077%)

$\varepsilon_{r,J_t^*}\% = [(\bar{\omega}_r)_{J_t^*=1} - (\bar{\omega}_r)_{J_t^*}] \times 100\%/(\bar{\omega}_r)_{J_t^*=1}$ for $r = 1-5$ and $J_t^* = 2, 3, 4$.

other than the point added masses. For the present example, the Exact method is not available for the determination of natural frequencies and the associated mode shapes of the beam, thus, only the PAM and FEM are used. Table 6(a) and Fig. 4(a), respectively, show the lowest five natural frequencies and mode shapes of the elastically supported beam with stiffness ratio $k_T^* = k_R^* = 1$ obtained from PAM and FEM, respectively. For comparison, the lowest five natural frequencies for the beam without any in-span lumped masses obtained from Table 2 are also inserted in Table 6. Besides, the draft ratio for Fig. 4 is also the same as that for Fig. 3, i.e., $L_1^* = L_1/L = 0.5$. Similarly, Table 6(b) and Fig. 4(b) show the corresponding ones of the fixedly supported beam.

From Tables 6(a) and (b) one sees that the two in-span lumped masses have the effect of reducing the lowest five natural frequencies of the elastically and fixedly supported beams to some degree except the second one ($\bar{\omega}_2$) of the elastically supported beam. This phenomenon may be

Table 6
The lowest five natural frequencies of the immersed beam with eccentricity $e = 0.5\,\text{m}$, tip-mass ratio $m_t^* = m_t/(\rho AL) = 0.1$, rotary-inertia ratio $J_t^* = J_t/(\rho AL^3) = 0.1$ and carrying two intermediate lumped masses $m_{53} = m_{57} = 0.5(\rho AL)\,\text{kg}$ located at $x_{53} = 13\,\text{m}$ and $x_{57} = 14\,\text{m}$, respectively, for the cases of draft ratios $L_1^* = L_1/L = 0$, 0.5, 1.0: (a) elastically supported with $k_T^* = K_R^* = 1.0$; (b) fixedly supported

Draft ratios $L_1^* = L_1/L$	Methods	Natural frequencies, $\tilde{\omega}_r$ (rad/s)				
		$\tilde{\omega}_1$ (or $\bar{\omega}_1$)	$\tilde{\omega}_2$ (or $\bar{\omega}_2$)	$\tilde{\omega}_3$ (or $\bar{\omega}_3$)	$\tilde{\omega}_4$ (or $\bar{\omega}_4$)	$\tilde{\omega}_5$ (or $\bar{\omega}_5$)
(a) Elastically supported with $k_T^* = K_R^* = 1.0$						
0.0	PAM	0.89746	3.33669	12.90022	46.17735	115.52633
	FEM	0.89746	3.33669	12.89966	46.16287	115.38645
	Table 2 (PAM)[a]	1.35219	3.45871	14.29530	51.49903	122.59260
0.5	PAM	0.89099	3.24742	12.60702	44.71613	112.60415
	FEM	0.89099	3.24742	12.60650	44.70220	112.47729
	Table 2 (PAM)	1.32839	3.39041	13.96915	49.91681	119.47037
1.0	PAM	0.87808	3.23895	12.58411	43.90325	109.83214
	FEM	0.87808	3.23895	12.58361	43.88903	109.72696
	Table 2 (PAM)	1.28691	3.37882	13.80756	48.98130	116.31352
(b) Fixedly supported						
0.0	PAM	2.59915	10.06158	43.72185	112.83035	200.50225
	FEM	2.59913	10.06134	43.71187	112.72485	198.60586
	Table 2 (Fixed)[b]	3.85344	11.68088	48.90633	119.83469	223.90777
0.5	PAM	2.59782	10.04429	42.32532	109.80158	195.74985
	FEM	2.59781	10.04406	42.31582	109.70780	194.03493
	Table 2 (Fixed)	3.84975	11.63030	47.36451	116.60237	217.03508
1.0	PAM	2.56978	9.98355	41.50510	107.06449	191.94800
	FEM	2.56977	9.98334	41.49567	106.97961	190.47930
	Table 2 (Fixed)	3.76627	11.36336	46.44083	113.49099	211.78150

[a]For the elastically supported immersed beam without in-span lumped masses studied in Table 2.
[b]For the fixedly supported immersed beam without in-span lumped masses studied in Table 2.

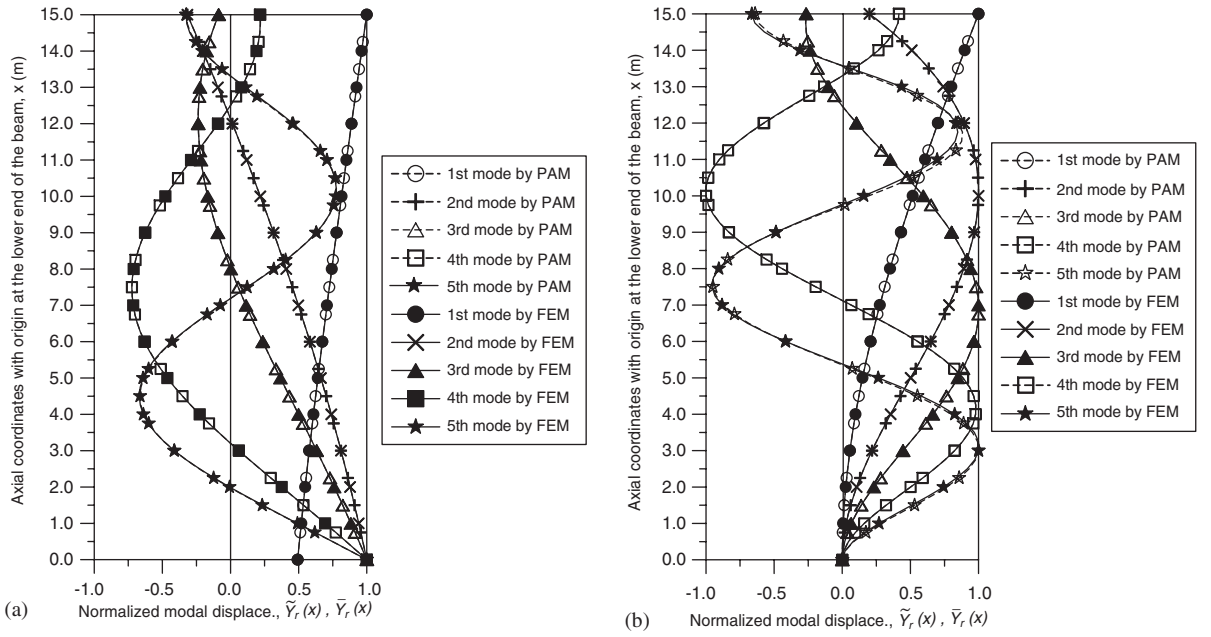

Fig. 4. The lowest five mode shapes of the immersed beam with eccentricity $e = 0.5\,\text{m}$, tip-mass ratio $m_t^* = m_t/(\rho AL) = 0.1$, rotary-inertia ratio $J_t^* = J_t/(\rho AL^3) = 0.1$, draft ratio $L_1^* = L_1/L = 0.5$ and carrying two intermediate lumped masses $m_{53} = m_{57} = 0.5(\rho AL)\,\text{kg}$ located at $x_{53} = 13\,\text{m}$ and $x_{57} = 14\,\text{m}$, respectively, obtained from PAM (------) and FEM (——) for (a) elastically supported with $k_T^* = K_R^* = 1.0$; (b) fixedly supported.

due to the fact that the two in-span lumped mass are located at stations 53 and 57, and these two stations are near the node of the second mode shape as one may see from Fig. 4(a).

In Figs. 4(a) and (b), the dashed curves with symbols, ○, +, △, □ and ☆ denote the 1st, 2nd, 3rd, 4th and 5th mode shapes obtained from the PAM, while the solid curves with ●, ×, ▲, ■ and ★ denote those obtained from the FEM. From the two figures one sees that the mode shapes obtained from FEM are very close to the corresponding ones obtained from PAM. Because the two in-span lumped masses reduce the lowest five natural frequencies of the beam of Section 6.2 to some degree, they also perceptibly change the associated lowest five mode shapes as one may see from Figs. 3 and 4.

7. Experiments and results

To check the foregoing theoretical results of this paper, several experiments were performed on the scale models of the fixed and elastically supported towers as shown in Figs. 5(a) and (b), respectively. The scale model of the fixed supported tower is composed of a uniform beam, a lumped mass and a rectangular heavy seat (about 60 kg weight). The assembly of the last three parts constitutes a unit, where the lower end of the uniform beam is fixed on the rectangular seat and its upper end is attached by the lumped mass (cf. Fig. 5(a)). The whole unit is fixed on the bottom of a water tank by using the screws on the rectangular seat. The diameter of the uniform

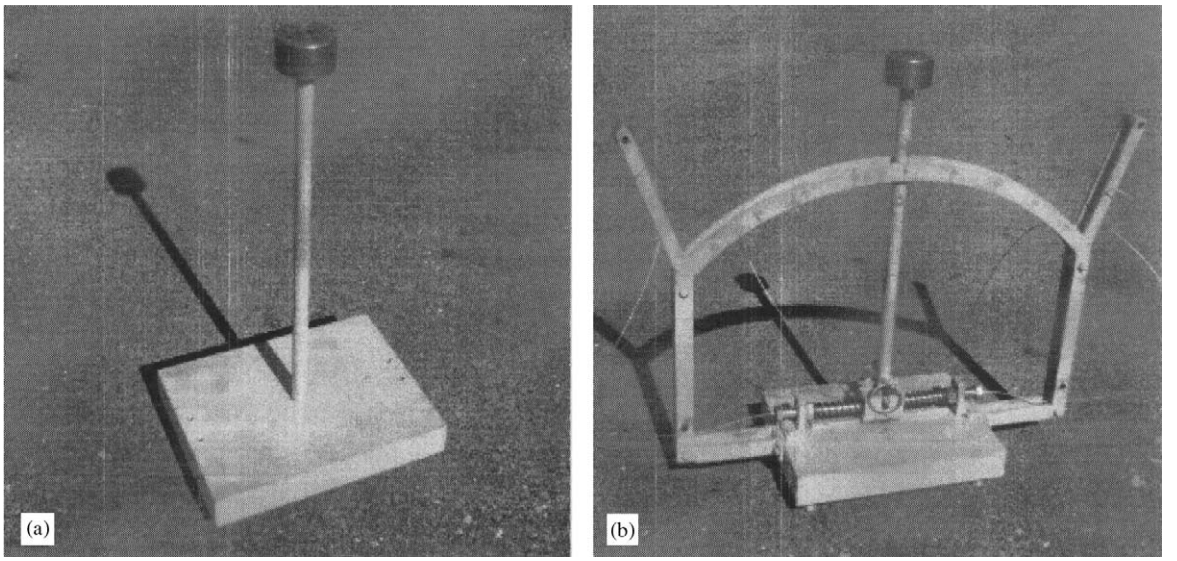

Fig. 5. Experimental scale models: (a) for fixed supported tower; (b) for elastically supported tower.

beam is $d = 0.025\,\mathrm{m}$, the total length is $L = 0.6\,\mathrm{m}$ and the total mass is $m_b = (7850 \times \pi \times 0.025^2 \times 0.6)/4 = 2.3120\,\mathrm{kg}$. The dimensions of the lumped mass are 0.08 m (diameter) × 0.046 m (height), thus its mass is $m_t = (7850 \times \pi \times 0.08^2 \times 0.046)/4 = 1.8151\,\mathrm{kg}$, its eccentricity is $e = 0.023\,\mathrm{m}$ and its rotary inertia is $J_t = 1.8151 \times (3 \times 0.04^2 + 0.046^2)/12 \approx 1.0461 \times 10^{-3}\,\mathrm{kg\,m^2}$. The weighted total mass of the beam (m_b) and that of the tip mass (m_t) are found to be very close to the last calculated values. The size of the water tank is 1.0 m (length) × 1.0 m (width) × 0.7 m (depth) (cf. Fig. 6). The dimensions for the model of the elastically supported tower are the same as those for the model of the fixed supported tower except the elastic supporting elements and the associated attachments at the lower end of the uniform beam (cf. Fig. 5(b)). In addition to the translational spring k_T on the right side of the lower end of the uniform beam as shown in Fig. 1, an identical spring on the left side of the lower end is also added (cf. Fig. 5(b)), so that when the lower end of the tower moves rightwards, the right spring is in compression and the left spring is in tension. On the contrary, when the lower end of the tower moves leftwards the last behaviors for the two translational springs are reverse.

If y_r denotes the rightward displacement of the lower end of the tower when it is subjected to a rightward force F_r and y_ℓ denotes the leftward one due to a leftward force F_ℓ, then the combined stiffness for the last two identical translational springs is determined by $k_T = 0.5[(F_r/y_r) + (F_\ell/y_\ell)] \approx 16,800\,\mathrm{N/m}$. Similarly, the combined stiffness for the two identical rotational springs set at the near side and far side of the lower end of the beam (cf. Figs. 1 and 5(b)) is determined by $k_R = 0.5[(M_c/\theta_c) + (M_{cc}/\theta_{cc})] \approx 162.9\,\mathrm{N\,m/rad}$, where θ_c denotes the rotational angle of the uniform beam about its lower end when the beam is subjected to a clockwise moment M_c and θ_{cc} denotes that when the beam is subjected to a counterclockwise moment M_{cc}. To assure the motion of the tower to be in the (vertical) xy-plane, a guiding mechanism is also constructed. The mechanism is composed of two identical curved beams set in

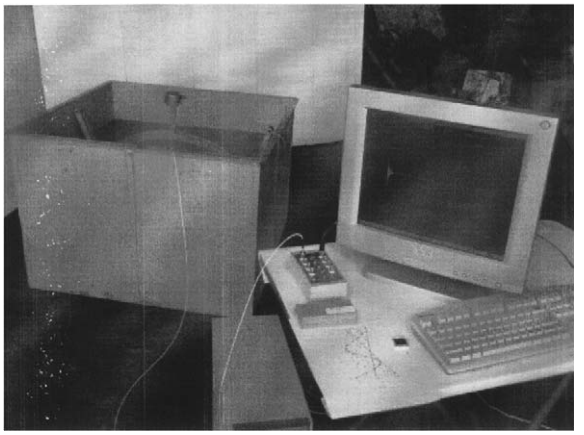

Fig. 6. The scale tower is tested in a water tank with 1.0 m (length) × 1.0 m (width) × 0.7 m (depth).

Table 7
Comparison between the lowest several natural frequencies for the models of "dry" tower obtained from experiments and those from exact method: (a) fixed supported; (b) elastically supported

Methods	Natural frequencies (rad/s)				
	$\bar{\omega}_1$	$\bar{\omega}_2$	$\bar{\omega}_3$	$\bar{\omega}_4$	$\bar{\omega}_5$
(a)					
Experiments	23	202	576	—	—
Exact	23.24191	211.96707	631.93665	1238.58971	2041.67399
(b)					
Experiments	2.0	23	203	576	—
Exact	2.00787	24.11113	215.98368	632.78805	1239.46669

parallel with the xy-plane and with the spacing between them to be slightly greater than the diameter of the uniform beam (0.025 m) so that the uniform beam may slide or rock in the spacing (cf. Fig. 5(b)). The average radius of each curved beam is 0.5 m with its center of curvature at the lower end of the beam. Furthermore, to assure the smooth translation of the lower end of tower in the y-direction, two small sheaves are also set at the lower end of the beam. The sheaves are constrained to roll along a rail on the rectangular seat.

The free vibrations of the scale towers are excited using the impact method and the responses are measured using an accelerometer. The signals are amplified and analyzed using the modal testing module of the I-DEAS computer package. For the model of "dry" towers, the lowest several natural frequencies are shown in Tables 7(a) and (b) for the fixed and elastically supported conditions, respectively. In either Tables 7(a) or (b), the 3rd row shows the frequencies obtained from current experiments and the 4th row shows the theoretical values obtained the exact method of this paper. It is seen that the agreement between the lower natural frequencies is reasonable. For the model of "wet" towers (with water depth $L_1 = 0.4$ m), the lowest several natural frequencies are shown in Tables 8(a) and (b) for the fixed and elastically supported conditions,

Table 8
Comparison between the lowest several natural frequencies for the models of "wet" tower (with water depth $L_1 = 0.4$ m) obtained from experiments and those from the exact method: (a) fixed supported; (b) elastically supported

Methods	Natural frequencies (rad/s)				
	$\bar{\omega}_1$	$\bar{\omega}_2$	$\bar{\omega}_3$	$\bar{\omega}_4$	$\bar{\omega}_5$
(a)					
Experiments	22.5	195	557	—	—
Exact	23.18904	204.19370	612.20640	1194.04910	1975.80194
(b)					
Experiments	1.9	22	196	559	—
Exact	1.99658	22.83291	207.56785	613.21454	1194.87726

respectively. Comparing the natural frequencies obtained from experiments with those from the exact method, one finds that the agreement between the corresponding lower ones is also reasonable.

8. Conclusions

1. A unified approach for the free vibration analysis of a (partially or fully) immersed uniform beam with either elastic or fixed support and carrying eccentric tip mass with rotary inertia is presented, based on which the formulation of the problem and the development of the computer programs are significantly simplified. Besides, the presented PAM derived from the unified approach is also practical for achieving the "approximate" solutions no matter whether or not the immersed beam is attached by a number of intermediate (in-span) realistic lumped masses in addition to the virtual point added masses due to surrounding water.
2. In reality, the lower end of an offshore tower is elastically (rather than fixed) supported. Therefore, it will be more reasonable to model the interactions between the lower end of the tower and the seabed (soil) by using a translational spring with stiffness k_T and a rotational spring with stiffness k_R. In such a situation, the dynamic characteristics of a fixed supported tower may be easily obtained from those of the elastically supported tower by setting the values of k_T and k_R to be very large (e.g., $k_T = k_R = 10^{16}$ N/m or N m).
3. Since the lowest two natural frequencies of an elastically supported tower are, respectively, associated with the two vibration modes major in the translational and rotational rigid-body motions of the tower, serious forced vibration responses of an elastically supported tower may be due to the lower frequency rigid-body motions rather than due to the higher frequency elastic vibrations of the tower.
4. The influences on the free vibration characteristics of an immersed beam of the tip mass m_t, the eccentricity e and the rotary inertia J_t are dependent on each other. The effect of m_t (or e) is dependent on the value of $m_t e$ (or $m_t e^2$). Because the magnitude of e will directly affect the magnitude of natural frequencies ($\bar{\omega}_r$), it will also indirectly influence the effect of J_t. Without tip mass (i.e., $m_t = 0$), the effect of eccentricity e is nil.

5. Increasing either the tip mass m_t or the rotary inertia J_t will reduce the natural frequencies of an immersed beam, $\bar{\omega}_r$. The last effect is the most predominant for the first natural frequency ($r = 1$) and decreases with increasing the order r of the vibration modes.
6. The first natural frequency ($\bar{\omega}_1$) of an immersed beam decreases with increasing the tip-mass eccentricity e, but this trend is reversed for the other higher natural frequencies $\bar{\omega}_r$ ($r = 2 - 4$).
7. The PAM is available for the free vibration analysis of an immersed beam with or without carrying any intermediate (in-span) lumped masses, but this is not true for the exact method. This is one of the reasons why the PAM is presented.

Acknowledgment

The experiments of this paper are supported by the National Science Council, Republic of China, under contract NSC 93-2611-E-006-017.

References

[1] P.A.A. Laura, J.L. Pombo, E.A. Susemihl, A note on the vibration of a clamped-free beam with a mass at the free end, *Journal of Sound and Vibration* 37 (2) (1974) 161–168.
[2] P.A.A. Laura, M.J. Maurizi, J.L. Pombo, A note on the dynamic analysis of an elastically restrained-free beam with a mass at the free end, *Journal of Sound and Vibration* 41 (4) (1975) 397–405.
[3] R.E. Rossi, P.A.A. Laura, D.R. Avalos, H.A. Larrondo, Free vibration of Timoshenko beams carrying elastically mounted concentrated masses, *Journal of Sound and Vibration* 165 (2) (1993) 209–223.
[4] M. Gurgoze, A note on the vibrations of restrained beams and rods with point masses, *Journal of Sound and Vibration* 96 (4) (1984) 461–468.
[5] M. Gurgoze, On the approximate determination of the fundamental frequency of a restrained cantilever beam carrying a tip heavy body, *Journal of Sound and Vibration* 105 (1986) 443–449.
[6] M. Gurgoze, On the eigenfrequencies of a cantilever beam with attached tip and a spring–mass system, *Journal of Sound and Vibration* 190 (2) (1996) 149–162.
[7] J.S. Wu, T.L. Lin, Free vibration analysis of a uniform cantilever beam with point masses by an analytical-and-numerical-combined method, *Journal of Sound and Vibration* 136 (2) (1990) 201–213.
[8] J.S. Wu, H.M. Chou, Free vibration analysis of a cantilever beam carrying any number of elastically mounted point masses with the analytical-and-numerical-combined method, *Journal of Sound and Vibration* 213 (2) (1998) 317–332.
[9] J.S. Wu, H.M. Chou, A new approach for determining the natural frequencies and mode shapes of a uniform beam carrying any number of sprung masses, *Journal of Sound and Vibration* 213 (2) (1998) 317–332.
[10] J.S. Wu, C.G. Huang, Free and forced vibrations of a Timoshenko beam with any number of translational and rotational springs and lumped masses, *Communications in Numerical Methods in Engineering* 11 (9) (1995) 713–756.
[11] H. Abramovich, O. Hamburger, Vibration of a cantilever Timoshenko beam with a tip mass, *Journal of Sound and Vibration* 148 (1) (1991) 162–170.
[12] H. Abramovich, O. Hamburger, Vibration of a cantilever Timoshenko beam with translational and rotational springs and with tip mass, *Journal of Sound and Vibration* 154 (1) (1992) 67–80.
[13] A. Uscilowska, J.A. Kolodziej, Free vibration of immersed column carrying a tip mass, *Journal of Sound and Vibration* 216 (1) (1998) 147–157.
[14] H.R. Oz, Natural frequencies of an immersed beam carrying a tip mass with rotatory inertia, *Journal of Sound and Vibration* 266 (2003) 1099–1108.

[15] P.A.A. Laura, R.H. Gutierrez, Vibration of an elastically restrained cantilever beam of varying cross-section with tip mass of finite length, *Journal of Sound and Vibration* 108 (1986) 123–131.
[16] T.W. Lee, Transverse vibrations of a tapered beam carrying a concentrated mass, *Journal of Applied Mechanics, ASME* June (1976) 366–367.
[17] H.H. Mabie, C.B. Rogers, Transverse vibrations of double-tapered beams with end support and with end mass, *Journal of the Acoustical Society of America* 55 (1974) 986–991.
[18] N.M. Auciello, Transverse vibration of a linearly tapered cantilever beam with tip mass of rotatory inertia and eccentricity, *Journal of Sound and Vibration* 194 (1) (1996) 25–34.
[19] J.Y. Chang, W.H. Liu, Some studies on the natural frequencies of immersed restrained column, *Journal of Sound and Vibration* 130 (3) (1989) 516–524.
[20] J.S. Wu, K.W. Chen, An alternative approach to the structural motion analysis of wedge-beam offshore structures supporting a load, *Ocean Engineering* 30 (14) (2003) 1791–1806.
[21] K. Nagaya, Transient response in flexure to general uni-directional loads of variable cross-section beam with concentrated tip inertias immersed in a fluid, *Journal of Sound and Vibration* 99 (1985) 361–378.
[22] K. Nagaya, Y. Hai, Seismic response of underwater members of variable cross section, *Journal of Sound and Vibration* 103 (1985) 119–138.
[23] Meirovitch, *Analytical Methods in Vibration*, MacMillan Company, London, 1967.
[24] F.H. Todd, *Ship Hull Vibration*, Edward Arnold Ltd, London, 1961.
[25] R.W. Clough, J. Penzien, *Dynamics of Structures*, McGraw-Hill, New York, 1975.
[26] J.D. Faires, R.L. Burden, *Numerical Methods*, PWS Publishing Company, Warsaw, 1993.